REPORT DOCUMENTATION PAGE

Form Approved
OMB No. 0704-0188

The public reporting burden for this collection of information is estimated to average 1 hour per response, including the time for reviewing instructions, searching existing data sources, gathering and maintaining the data needed, and completing and reviewing the collection of information. Send comments regarding this burden estimate or any other aspect of this collection of information, including suggestions for reducing the burden, to the Department of Defense, Executive Services and Communications Directorate (0704-0188). Respondents should be aware that notwithstanding any other provision of law, no person shall be subject to any penalty for failing to comply with a collection of information if it does not display a currently valid OMB control number.

PLEASE DO NOT RETURN YOUR FORM TO THE ABOVE ORGANIZATION.

1. REPORT DATE *(DD-MM-YYYY)*	2. REPORT TYPE	3. DATES COVERED *(From - To)*
xx-03-2004		

4. TITLE AND SUBTITLE
Decadal Current Variations in the Southwestern Japan/East Sea

5a. CONTRACT NUMBER

5b. GRANT NUMBER

5c. PROGRAM ELEMENT NUMBER
0602435N

6. AUTHOR(S)
William J. Teague, Gregg A. Jacobs, Douglas Mitchell, M. Wimbush, D.R. Watts

5d. PROJECT NUMBER

5e. TASK NUMBER

5f. WORK UNIT NUMBER
73-7507-03-5

7. PERFORMING ORGANIZATION NAME(S) AND ADDRESS(ES)
Naval Research Laboratory
Oceanography Division
Stennis Space Center, MS 39529-5004

8. PERFORMING ORGANIZATION REPORT NUMBER
NRL/JA/7330-03-18

9. SPONSORING/MONITORING AGENCY NAME(S) AND ADDRESS(ES)
Office of Naval Research
800 N. Quincy St.
Arlington, VA 22217-5660

10. SPONSOR/MONITOR'S ACRONYM(S)
ONR

11. SPONSOR/MONITOR'S REPORT NUMBER(S)

12. DISTRIBUTION/AVAILABILITY STATEMENT
Approved for public release, distribution is unlimited.

13. SUPPLEMENTARY NOTES

14. ABSTRACT
Absolute geostrophic velocities were calculated along TOPEX/Poseidon (T/P) groundtracks located in the Ulleung Basin of the southwestern Japan/East Sea (JES) from a combined analysis of nearly a decade of T/P data and two years of pressure-gauge-equipped inverted echo sounder (PIES) data obtained during the United States Office of Naval Research's JES Program. Geostrophic velocities have been calculated daily for the Ulleung Basin from June 1999 to July 2001 from a three-dimensional mapping of temperature and salinity produced by PIES data interpreted via the Gravest Empirical Mode (GEM) technique combined with the Navy's Modular Ocean Data Assimilation System (MODAS). These velocities were then used to convert T/P velocity anomalies to absolute velocities for the T/P time period of 1993 to 2002. Current intensities and variabilities associated with the East Korean Warm Current, Ulleung Warm Eddy, and Offshore Branch are examined. Spatial and temporal variations of the sea surface circulation are strong. Intensification of the currents generally occurred during the fall season. The flow pattern in individual years differed greatly from year to year and differed from climatology in important qualitative ways.

15. SUBJECT TERMS
Japan Sea, Ulleung Basin, Currents, TOPEX, PIES, East Korean Warm Current, Ulleung Warm Eddy, offshore branch, marginal sea oceanography

16. SECURITY CLASSIFICATION OF:			17. LIMITATION OF ABSTRACT	18. NUMBER OF PAGES	19a. NAME OF RESPONSIBLE PERSON
a. REPORT	b. ABSTRACT	c. THIS PAGE			William J. Teague
Unclassified	Unclassified	Unclassified	UL	11	19b. TELEPHONE NUMBER *(Include area code)* 228-688-4734

Journal of Oceanography, Vol. 60, pp. 1023 to 1033, 2004

Decadal Current Variations in the Southwestern Japan/East Sea

WILLIAM J. TEAGUE[1]*, GREGG A. JACOBS[1], DOUGLAS A. MITCHELL[1], MARK WIMBUSH[2] and D. RANDOLPH WATTS[2]

[1]*Naval Research Laboratory, Stennis Space Center, MS 39529-5004, U.S.A.*
[2]*GSO, University of Rhode Island, Narragansett, RI 02882-1197, U.S.A.*

(Received 17 September 2003; in revised form 11 March 2004; accepted 15 March 2004)

Absolute geostrophic velocities were calculated along TOPEX/Poseidon (T/P) groundtracks located in the Ulleung Basin of the southwestern Japan/East Sea (JES) from a combined analysis of nearly a decade of T/P data and two years of pressure-gauge-equipped inverted echo sounder (PIES) data obtained during the United States Office of Naval Research's JES Program. Geostrophic velocities have been calculated daily for the Ulleung Basin from June 1999 to July 2001 from a three-dimensional mapping of temperature and salinity produced by PIES data interpreted via the Gravest Empirical Mode (GEM) technique combined with the Navy's Modular Ocean Data Assimilation System (MODAS). These velocities were then used to convert T/P velocity anomalies to absolute velocities for the T/P time period of 1993 to 2002. Current intensities and variabilities associated with the East Korean Warm Current, Ulleung Warm Eddy, and Offshore Branch are examined. Spatial and temporal variations of the sea surface circulation are strong. Intensification of the currents generally occurred during the fall season. The flow pattern in individual years differed greatly from year to year and differed from climatology in important qualitative ways.

Keywords:
- Japan Sea,
- Ulleung Basin,
- currents,
- TOPEX,
- PIES,
- East Korean Warm Current (EKWC),
- Ulleung Warm Eddy,
- offshore branch,
- marginal sea oceanography.

1. Introduction

The Japan/East Sea[§] (JES) is a deep, semi-enclosed marginal sea surrounded by Korea, Russia, and Japan and is connected with the East China Sea to the south by the Korea/Tsushima Strait (KTS), with the Pacific Ocean to the east by the Tsugaru Strait, and with the Sea of Okhotsk to the north by the Soya and Tartar Straits. Maximum depth in the JES is about 3700 m, occurring in the deep central Japan Basin in the northern JES. The Ulleung Basin, located in the southwestern JES, has a maximum depth of approximately 2200 m. Connected to the Ulleung Basin, the KTS is oriented in a southwest-northeast direction and consists of a western channel and an eastern channel. While most of the KTS is about 100 m deep, a narrow channel about 130 m deep exists to the west of Tsushima Island.

Warm and salty water enters the Ulleung Basin of the JES through the KTS as the Tsushima Warm Current (TWC). Although the TWC is confined to approximately the top 200 m in the JES because of the shallow sill depth in the KTS, the TWC is thought to impact the formation of fronts and eddies and to have a major effect on the circulation in the Ulleung Basin. Currents in the Ulleung Basin are important in the transfer of dynamic, thermodynamic, biological, and passive tracer properties into the entire JES. Hence, a great deal of effort has been devoted to measuring the transport through the KTS and to map the circulation patterns in the Ulleung Basin. However, there have been few direct measurements of currents in the Ulleung Basin. The main focus of direct current measurements has been on the TWC in the KTS (Mizuno *et al.*, 1989; Egawa *et al.*, 1993; Isobe *et al.*, 1994, 2002; Katoh *et al.*, 1996; Teague *et al.*, 2002).

The historical interpretation by Suda and Hidaka (1932) and by Uda (1934) portrays the TWC as splitting into three branches upon entering the JES (Fig. 1(a)). The first branch (Nearshore Branch) enters the JES through the eastern channel and flows along the Japanese coast, confined shoreward of the 200 m isobath. The second branch (Offshore Branch; OB), generally thought to enter the JES through the western channel (Suda and Hidaka, 1932; Byun and Chang, 1984), flows eastward along the

* Corresponding author. E-mail: teague@nrlssc.navy.mil

§ The Editor-in-Chief does not recommend the usage of the term "East Sea" in place of "Japan Sea".

Copyright © The Oceanographic Society of Japan.

20050225 041

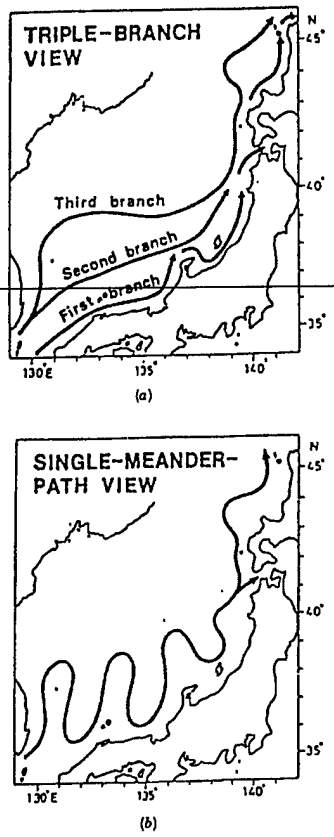

Fig. 1. Theorized paths of the Tsushima Current in the JES: (a) triple branch theory, (b) single-meander theory (adapted from Naganuma, 1973).

continental shelf break. The third (East Korean Warm Current; EKWC) branch enters the JES through the western channel and flows northward along the continental slope off the east coast of Korea. The EKWC is important since it transports heat and salt northward and is the source of the warm surface layer that spreads throughout the Ulleung Basin. The EKWC meets the southward flowing North Korean Cold Current and separates from the coast at about 37–38°N. Some eastward flow is observed along the Subpolar Front and a large meander often forms in the vicinity of Ulleung Island. The interior of the meander crest forms the Ulleung Warm Eddy (UWE) (Ichiye and Takano, 1988; Kang and Kang, 1990; Kim *et al.*, 1991). Furthermore, Lie *et al.* (1995) suggest that the EKWC splits into two branches with the main branch meandering around Ulleung Island and a minor branch flowing northeastward to contribute to the Subpolar Front. Paths of satellite-tracked drifters have demonstrated that the behavior of the TWC in the JES is very complicated in both space and time (Beardsley *et al.*, 1992; Lee *et al.*, 2000).

The branches have been viewed as permanent features from analysis of observational data and models (Kawabe, 1982a, b; Yoon, 1982a, b; Morimoto and Yanagi, 2001). However, occasional absence of the EKWC, or third branch, has been suggested by anomalously cold waters off the east coast of Korea (Hong *et al.*, 1984; Kim and Legeckis, 1986). Cho and Kim (1996) suggest the absence of the EKWC in winter using satellite images with concurrent hydrographic data. The absence of the EKWC, however, was also found in summer or fall (Hong *et al.*, 1984; Katoh, 1994; Mitchell *et al.*, 2004a). In contrast, Kawabe (1982a) suggests that the first branch at least exists during spring and summer, the second branch exists only during summer, while the third branch (the EKWC) exists throughout the year. Hase *et al.* (1999) observed the first and second branches using acoustic Doppler current profiler (ADCP) and historical temperature data and noted that the second branch could not always be detected around the shelf break due to eddy activity. Teague *et al.* (2003) suggested that much of the eddy activity northeast of Tsushima Island is due to the island wake. As an alternative to the branching view, Moriyasu (1972) proposed that the TWC enters the JES as a single meandering current that episodically sheds eddies (Fig. 1(b)). Others have suggested that both branching and single meandering current patterns appear alternately (Naganuma, 1985; Kim and Legeckis, 1986).

Long-term measurements of currents using moorings are difficult to make in the Ulleung Basin because of intense fishing. Crabbers lay crab lines, 1000 m and longer, on the bottom at depths of over 1000 m. Hence, most observations of currents in the Ulleung Basin have been indirect, using hydrographic density measurements and the geostrophic method. Even the rare transects that used direct measurements to reference the geostrophic profiles, such as from ship-mounted ADCPs, lack temporal and spatial coverage. The variety of estimated circulation patterns cited earlier probably arose not only because of the limited surveys but also because the circulation patterns varied from year to year. Hence, it is not surprising that the current structure within the Ulleung Basin has been obscure. Recently Mitchell *et al.* (2004a) observed at least five distinct flow patterns in the Ulleung Basin during a two-year period, using an array of pressure-gauge equipped inverted echo sounders (PIES) to generate three-dimensional (x, y, z) daily maps of temperature, density, and current.

Satellite altimetry can provide nearly global observations of sea surface height (SSH) variability. In the JES, SSH variability was used by Morimoto *et al.* (2000) to describe the temporal and spatial variation of warm and cold eddies and by Hirose and Ostrovskii (2000) to examine intraseasonal and annual variability of the currents. However, the use of altimeter data to estimate that part of

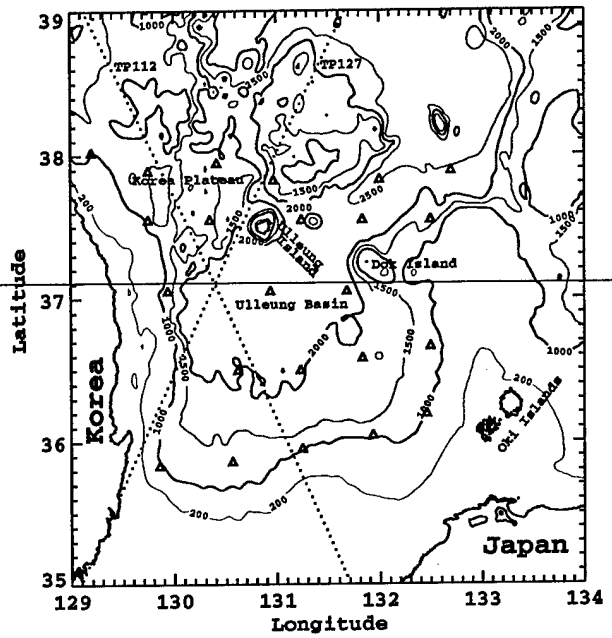

Fig. 2. Locations of the PIES moorings (triangles) are shown. T/P tracks 112 and 127 are indicated by dotted lines. Depths are in meters. Bathymetry is from a 1-minute resolution data set available from the Laboratory for Coastal and Ocean Dynamics Studies, Sung Kyun Kwan University (Choi, 1999).

the surface topography due to absolute ocean currents has remained elusive, because it is difficult to separate oceanographic features from the much larger but imprecisely known spatial variations in the geoid. If the altimetry time series is very long in time and the distribution of the currents is random, then the geoid can be estimated simply by the long-term mean of the altimetric height time series. Usually, the long-term mean circulation will contaminate the inferred geoid. Investigators have therefore sought other ways to reference the SSH, from which in principle the geoid would be known along a particular ground track for all times. Morimoto and Yanagi (2001) referenced SSH variability with the mean surface height calculated from a numerical model and examined the absolute current variability in the JES. Mitchell *et al.* (1990) and Carnes *et al.* (1990) obtained geoid accuracies of 10 to 20 cm rms error using airborne expendable bathythermograph surveys conducted simultaneously with altimeter measurements. Teague *et al.* (1997) estimated the geoid across the Kuroshio Extension near its separation point from Japan to 8 cm rms error through an analysis of coincident SSH measurements from PIESs and TOPEX/Poseidon (T/P). Long time series of both in situ and altimeter sampling are generally necessary to reduce noise from single-pass measurements.

There are now about 10 years of T/P data available for analysis. PIES data have been collected over the Ulleung Basin between June 1999 and July 2001 (Fig. 2). A new method which extends the Gravest Empirical Mode (GEM) technique (Meinen and Watts, 2000; Watts *et al.*, 2001) through combined analysis with the Navy's Modular Ocean Data Assimilation System (MODAS) static climatology (Fox *et al.*, 2002) is used to interpret the PIES data and to produce maps of temperature, density, and geostrophic velocity. The GEM/MODAS technique, has been fully described by Mitchell *et al.* (2004b). Geostrophic currents are used here to convert velocity anomalies computed from T/P to absolute currents. Currents are analyzed along two T/P tracks (Fig. 2) for the time period November, 1993 through February, 2002. The EKWC, OB, and UWE are observed along these tracks. Their positions and strengths, and corresponding signatures, change significantly from year to year. A new perspective is presented for the circulation in the southwestern JES.

2. Measurements

The PIES measurements in the Ulleung Basin were part of the United States Office of Naval Research JES (Japan/East Sea) program. A two-dimensional array of 23 PIES was deployed for two years, from June 1999 to July 2001 (Fig. 2). The PIES recorded hourly observations of vertical acoustic travel time and pressure from which profiles of temperature and salinity are derived. The GEM/MODAS technique interprets the PIES data in terms of the measured departures from the MODAS climatology at PIES sites due to mesoscale eddies and interannual variability. Using a 500 dbar reference level, acoustic travel time measurements were objectively mapped onto a 1/8° × 1/8° grid, approximately spanning 35.8°N to 38.0°N, 129.8°E to 132.5°E. Vertical profiles of temperature, salinity, and specific volume anomaly were calculated at each grid point. Geostrophic velocities relative to 500 dbar were then calculated at a daily interval. Thus, two-year, three-dimensional (x, y, z) time series of temperature, salinity, and velocity were produced for the entire Ulleung Basin. Details of the processing and more on the GEM/MODAS technique can be found in Mitchell *et al.* (2004a, b).

T/P was launched on 10 August 1992 as a joint effort by National Aeronautics and Space Administration (NASA) and the French Space Agency, Centre National d'Etudes Spatiales (CNES), for studying global ocean circulation (Fu *et al.*, 1994). The T/P data are obtained from the Geophysical Data Records (GDRs) processed at the Physical Oceanography Distributed Active Archive Center (PODAAC) at the Jet Propulsion Laboratory. T/P has a repeat period of 9.92 days and a cross-track separa-

tion of about 225 km at 36°N. T/P data are corrected for the effects of wet troposphere from an onboard water vapor radiometer, dry troposphere, ionosphere from the dual-frequency altimeter, inverse barometer, and electromagnetic bias. Tidal contamination is eliminated using the tide model, GOT00.2, described by Schrama and Ray (1994). This model is demonstrably more accurate than models described by Schwiderski (1980) and by Cartwright and Ray (1991). After removing the tide model solution, residual tide variability is eliminated using a least squares fit of eight principle tide frequencies. The height data are interpolated along track to a reference ground track produced at the Colorado Center for Astrodynamics Research, resulting in about 7-km along-track resolution.

The satellite altimeter measures the distance between the satellite and the ocean surface. When combined with precise orbit determination, this provides a measurement of sea level, the height of the ocean surface above the Earth's reference ellipsoid. The error of the altimeter measurements is estimated to be 4.8 cm rms (Fu *et al.*, 1994). In the absence of currents and external forcing, sea level coincides with the geopotential surface known as the geoid. The altimeter sea level measurement is the sum of the geoid, which is constant in time, plus sea surface height departures due to oceanographic features such as currents and tides. However, the spatial variations of the geoid are one to two orders of magnitude larger than SSH spatial variations. Thus separation of the geoid from the mean sea level is not sufficiently accurate for absolute surface velocity estimation from altimeter data alone. Without an accurate geoid from independent measurements, only temporal variations of SSH about mean sea level are observable. Thus, the main focus of altimetry traditionally has been SSH variability and associated surface velocity anomalies.

Two T/P tracks pass through the Ulleung Basin, along which the geoid can be calculated using the PIES data. The total anomaly of SSH measured by the PIES data is

$$H_{IES} = H_{bcl} + H_{btr}, \tag{1}$$

where *bcl* and *btr* refer to baroclinic and barotropic components of the height field. Analysis of pressure records reveals that the barotropic component of the height field is small, generally less than about 1 cm rms. Hence, in the Ulleung Basin, SSH is dominated by the baroclinic component, and thus it is reasonable to estimate H_{IES} from H_{bcl} here. The primary source of baroclinic error in H_{IES} is caused by temperature and salinity variations in the upper 400 m of the water column. This error, estimated using over 2200 hydrocasts, is about 2.5 cm for the Ulleung Basin. Thus the total rms error in PIES SSH, estimated from baroclinic and barotropic errors, is less than 3 cm. Using sea surface height anomaly, H_{IES}, estimated from PIES data and sea surface height, $H_{T/P}$, measured by T/P, an estimate of the geoid, G, is given by:

$$G = \overline{H_{T/P} - H_{IES}}^{2yr} = \overline{H_{T/P}}^{2yr} - \overline{H_{IES}}^{2yr}, \tag{2}$$

where the means are computed for T/P sample times over the 2-year PIES recording period.

Therefore

$$H_{IES} = H_{T/P} - G = H_{T/P} - \overline{H_{T/P}}^{2yr} + \overline{H_{IES}}^{2yr}. \tag{3}$$

Usually sea surface height anomaly, *SSHA*, is computed from T/P using the average T/P SSH computed over the entire T/P recording period (now over 10 years), with

$$SSHA = H_{T/P} - \overline{H_{T/P}}^{tot} \tag{4}$$

and

$$\overline{SSHA}^{2yr} = \overline{H_{T/P}}^{2yr} - \overline{H_{T/P}}^{tot}. \tag{5}$$

Then

$$H_{IES} = SSHA - \overline{SSHA}^{2yr} + \overline{H_{IES}}^{2yr} = SSHA + G^*, \tag{6}$$

where we define

$$G^* = \overline{H_{IES}}^{2yr} - \overline{SSHA}^{2yr} = \overline{H_{T/P}}^{tot} - G. \tag{7}$$

Gradients in G^* arise from the mean geostrophic surface currents. The standard error, E, in the estimate of G^* is

$$E = \frac{\sigma(G^*)}{N^{1/2}}, \tag{8}$$

where σ is the standard deviation and N is the number of observations at each T/P ground point. Average rms values for G^* along T/P 112 and 127 (Fig. 2) are 3.8 and 5.4 cm, respectively. Values of G^* with standard deviation at the ground points along the T/P tracks 112 and 127 are listed in Tables 1 and 2. Over the two year PIES deployment period, about 70 satellite passes contribute to estimating the geoid, which reduces data noise to an error generally better than 1 cm rms.

Therefore, geostrophic velocity anomalies computed from T/P SSHA can be adjusted to absolute geostrophic velocity by including the velocity component arising from G^*, computed from the difference in heights between the

Table 1. T/P Track 112 G^* and standard deviation.

Lat.	Lon.	G^* (m)	sigma (m)
35.890	131.167	0.707	0.024
35.936	131.138	0.703	0.024
35.983	131.110	0.700	0.024
36.029	131.081	0.698	0.025
36.075	131.052	0.694	0.026
36.121	131.023	0.690	0.027
36.168	130.994	0.687	0.029
36.214	130.965	0.683	0.028
36.260	130.936	0.679	0.028
36.306	130.907	0.676	0.028
36.353	130.878	0.673	0.029
36.399	130.849	0.672	0.030
36.445	130.820	0.672	0.031
36.491	130.791	0.670	0.033
36.537	130.761	0.671	0.034
36.583	130.732	0.672	0.038
36.629	130.703	0.671	0.042
36.676	130.673	0.670	0.046
36.722	130.644	0.671	0.050
36.768	130.615	0.670	0.053
36.814	130.585	0.667	0.054
36.860	130.556	0.663	0.056
36.906	130.526	0.661	0.058
36.952	130.496	0.660	0.059
36.998	130.467	0.657	0.059
37.044	130.437	0.652	0.058
37.090	130.407	0.649	0.056
37.136	130.378	0.645	0.054
37.182	130.348	0.639	0.053
37.228	130.318	0.635	0.051
37.274	130.288	0.629	0.049
37.320	130.258	0.624	0.046
37.366	130.228	0.619	0.043
37.412	130.198	0.612	0.040
37.458	130.168	0.606	0.038
37.504	130.138	0.602	0.037
37.550	130.108	0.599	0.034
37.596	130.078	0.597	0.032
37.642	130.048	0.594	0.031
37.688	130.017	0.593	0.029
37.734	129.987	0.590	0.030
37.780	129.957	0.588	0.030
37.825	129.926	0.588	0.030
37.871	129.896	0.586	0.030
37.917	129.865	0.585	0.029
37.963	129.835	0.582	0.039
38.009	129.804	0.583	0.041
38.055	129.774	0.585	0.038
38.101	129.743	0.583	0.029

Table 2. T/P Track 127 G^* and standard deviation.

Lat.	Lon.	G^* (m)	sigma (m)
36.518	130.024	0.559	0.056
36.564	130.054	0.564	0.055
36.610	130.083	0.569	0.055
36.657	130.112	0.575	0.054
36.703	130.142	0.582	0.055
36.749	130.171	0.588	0.054
36.795	130.200	0.593	0.052
36.841	130.230	0.598	0.053
36.887	130.260	0.604	0.056
36.933	130.289	0.605	0.058
36.979	130.319	0.608	0.060
37.025	130.348	0.608	0.062
37.071	130.378	0.608	0.063
37.117	130.408	0.606	0.064
37.163	130.438	0.602	0.064
37.209	130.467	0.599	0.065
37.255	130.497	0.597	0.065
37.301	130.527	0.590	0.063
37.347	130.557	0.585	0.061
37.393	130.587	0.581	0.058
37.439	130.617	0.575	0.056
37.485	130.647	0.572	0.055
37.531	130.677	0.567	0.053
37.577	130.708	0.564	0.052
37.623	130.738	0.560	0.051
37.669	130.768	0.557	0.049
37.715	130.798	0.553	0.047
37.761	130.829	0.550	0.045
37.807	130.859	0.547	0.045
37.853	130.889	0.545	0.045
37.898	130.920	0.542	0.044
37.944	130.950	0.544	0.045
37.990	130.981	0.537	0.041

2-year mean dynamic height from the PIES data and the 2-year mean *SSHA* from T/P. The referenced geostrophic height which is used to calculate absolute geostrophic velocity from T/P SSHA is given by

$$SSH_r = SSHA + G^*. \tag{9}$$

The rms difference between SSH_r and H_{IES} during the PIES measurement period is 5.6 cm. Much of this difference is attributed to noise in the altimetry data. The velocity adjustments (mean geostrophic velocities) for T/P tracks 112 and 127 that arise from G^* are shown in Fig. 3 with corresponding means of 5 cm/s and 1 cm/s, and standard deviations of 3.6 cm/s and 7.8 cm/s, respectively. These adjustments can be applied to T/P velocity anomalies to obtain absolute velocities. The absolute velocity can be considerably different from the velocity anomaly computed from SSHA.

3. Current Observations

The T/P time period for this analysis is from December 1992 through February 2002. Current maps, produced from daily PIES analyses, are available for comparison

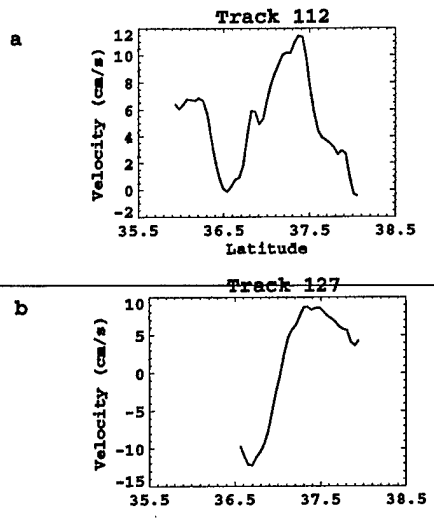

Fig. 3. Mean geostrophic velocities along T/P tracks 112 (a) and 127 (b). T/P velocity anomalies along track can then be adjusted to absolute velocities.

with the T/P currents for the period June 1999 through July 2001. Two T/P tracks (112 and 127) (Fig. 2) fall within the PIES gridded data domain. T/P 127 is located in the western half of the basin and passes within about 10 km of Ulleung Island but is oriented southwest to northeast. Such an orientation is not good for observing the EKWC between 36.5°N and 37.0°N since the current tends to flow parallel to this track and the corresponding cross-track geostrophic velocity component would be small. However, the UWE and/or the EKWC should be observable between 37°N and 38°N, but would not be distinguishable from one another. T/P 112, also located in the western half of the Ulleung Basin, is oriented northwest to southeast and passes within about 40 km southwest of Ulleung Island. This orientation is suitable for observing the UWE, EKWC, and the OB. Hence, T/P 112 is the main focus for this analysis.

Absolute current velocities and referenced SSHs for almost a decade of T/P data are shown for T/P 112 in Fig. 4. Positive velocities are towards the northeast and negative velocities are towards the southwest. High variability is found in the seasonal, annual, and interannual current and SSH fields. Locations of the EKWC (northeastward flow), OB (northeastward flow), and UWE (northeastward and southwestern flow pair) are marked in the velocity section. The OB is identified up to about 36.1°N, the EKWC is generally located between about 36.2°N and 37.4°N, and the UWE is seen between 36.3°N and 38°N along T/P 112. It is often difficult to distinguish the EKWC from the OB and the EKWC from the UWE near its southern and northern manifestations, respectively, along T/P 112.

The surface velocities in Fig. 4, lower panel, provide clearer signatures of circulation features than do the SSH transects alone on T/P 112 (Fig. 4, upper panel). SSH along T/P 112 can vary by over 50 cm between seasons. Highs in SSH occur during fall during each of the years but vary greatly with latitude between years. The weakest fall maximum occurs during the year 2000. The annual cycle consisting of a fall maximum is clearly seen in the monthly average of the heights over the T/P period (Fig. 5). Clearly, the average annual cycle does not reflect individual years.

Absolute current velocities and referenced SSHs for T/P 127 are shown in Fig. 6. In this case, positive velocities are towards the southeast and negative velocities are towards the northwest. In general, currents are difficult to interpret across T/P 127 due to the track orientation, but the stronger current signatures across this track help to interpret the currents across T/P 112. As also observed along T/P 112, strong UWE signatures are similarly found along T/P 127 during 1993 and 2000. A weaker fall maximum is found in the average annual cycle (not shown). Interestingly, maxima in SSH during fall 1999 and fall 2001, which occur at the beginning of the PIES measurement period and just after the PIES period, respectively, suggest a redistribution of flow between the UWE and EKWC.

Currents vary greatly from one interval to another throughout the decade. A strong UWE signature is apparent over the two-year period from 1999 to 2001 (Fig. 4, lower panel). The eddy signature consists of a northeastward flow between about 37.0°N and 37.8°N, and a reverse southwestward flow between about 36.3°N and 37.5°N. Strong northeastward flows along the southern boundary of the T/P current section (for example, 1993–1994, 1996, and 2000) are associated with the OB. Northeastward flow between approximately 36.25°N and 37.5°N is likely EKWC flow. Northeastward flow north of 37.25°N can be either associated with the UWE or the EKWC. The banded structure of negative velocities, sloping upward from left to right, and most apparent prior to the PIES deployment period but weakly seen during February 2000, are associated with a more eastward displaced, smaller UWE, and a northwestward EKWC. The negative velocities south of 36.5°N are likely associated with eddies.

Daily surface current and temperature (100 m) maps were made from the PIES data for the Ulleung Basin. Comparisons of these maps with independent temperature measurements from the Korean Oceanographic Research and Development Institute, Korean Fisheries Department, and the Japan Oceanographic Center independently confirmed that these maps accurately depicted the temperature structure in the Ulleung Basin (Mitchell *et al.*, 2004b). A better understanding of the flow across T/

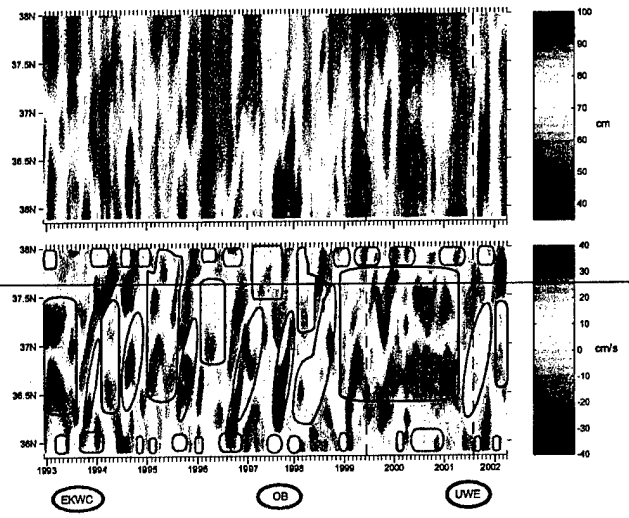

Fig. 4. Absolute-velocity time section (lower panel) and referenced geostrophic surface height (upper panel) along track 112 in the Ulleung Basin are shown for 1993 through 2002. Positive velocities are northeastward and negative velocities are southwestward. Manifestations of the East Korean Warm Current (EKWC), Ulleung Warm Eddy (UWE), and Offshore Branch (OB) are indicated on the velocity section. The PIES measurement period is located between the two dashed vertical lines.

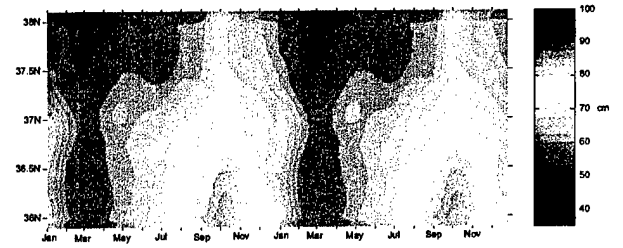

Fig. 5. Average annual cycle formed by the monthly average of the referenced geostrophic surface heights over the T/P 112 period. For display purposes, two identical years are shown.

P 112 (Fig. 4) can be formed by comparisons of these maps with the currents observed across the track during the PIES measurement time period (June 1999 to July 2001) (Fig. 4). Several representative temperature and current vector maps along with corresponding geostrophic velocities along T/P 112 are shown in Fig. 7. On July 2, 1999 (Fig. 7(a)) the EKWC is associated with the strong temperature gradient near the Korean coast between 37°N and 38°N. Circulation in the interior of the Ulleung Basin is weakly cyclonic but there are indications of the formation of the anticyclonic UWE, centered near 36.8°N.

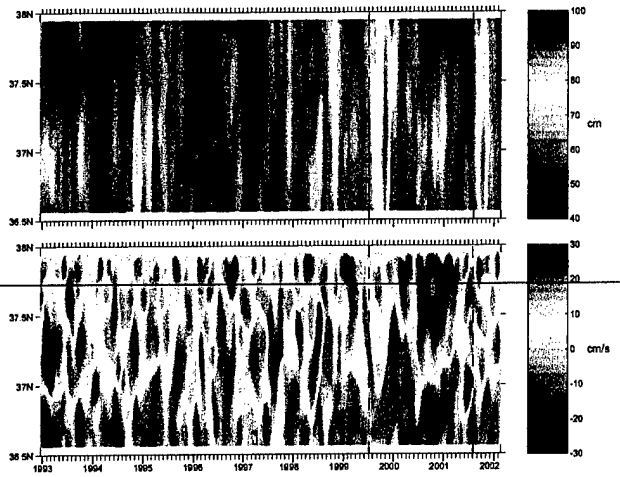

Fig. 6. Absolute-velocity time section (lower panel) and referenced geostrophic surface height (upper panel) along track 127 in the Ulleung Basin are shown for 1993 through 2002. Positive velocities are southeastward and negative velocities are northwestward. The PIES measurement period is located between the two dashed vertical lines.

Velocity across the T/P 112 section is positive due to the northward flowing EKWC observed between 37°N and 38°N, negative between 36.2°N and 37°N due to the westward portion of the basin cyclonic flow, and positive between 35.9°N and 36.2°N, likely due to a combination of the eastward portion of the cyclonic flow and OB. By August 30 (Fig. 7(b)), the UWE, centered near 36.5°N, is clearly formed. Large positive and negative velocities are found in the T/P 112 section in August–September 1999, which correspond to intensification of the anticyclonic flow observed in the PIES maps for the same time period. The UWE fills the entire northern half of the basin and an OB occurs at about 36°N on December 27, 1999 (Fig. 7(c)). The T/P section (Fig. 4) also shows the positive flows associated with the EKWC, UWE, and OB, and negative flow associated with the UWE. The EKWC is not separable from the UWE in the T/P current section.

Mitchell *et al.* (2004a) reported that the EKWC was absent from June to November of 2000. Representative currents for this time period are shown in the September 11 map (Fig. 7(d)). Across the T/P 112 section (Fig. 4) for the June to November, 2000 time period, there is negative flow between about 36.3°N and 36.8°N and north of 37.75°N, and there is an intensification of positive flow along the southern boundary. This flow scenario in the T/P section is also suggestive of a missing EKWC. A difficult pattern to interpret begins in April of 2001 and continues through October. Mitchell *et al.* (2004a) determined that this pattern resulted from a meander forming from an UWE elongation that merged with the OB. For exam-

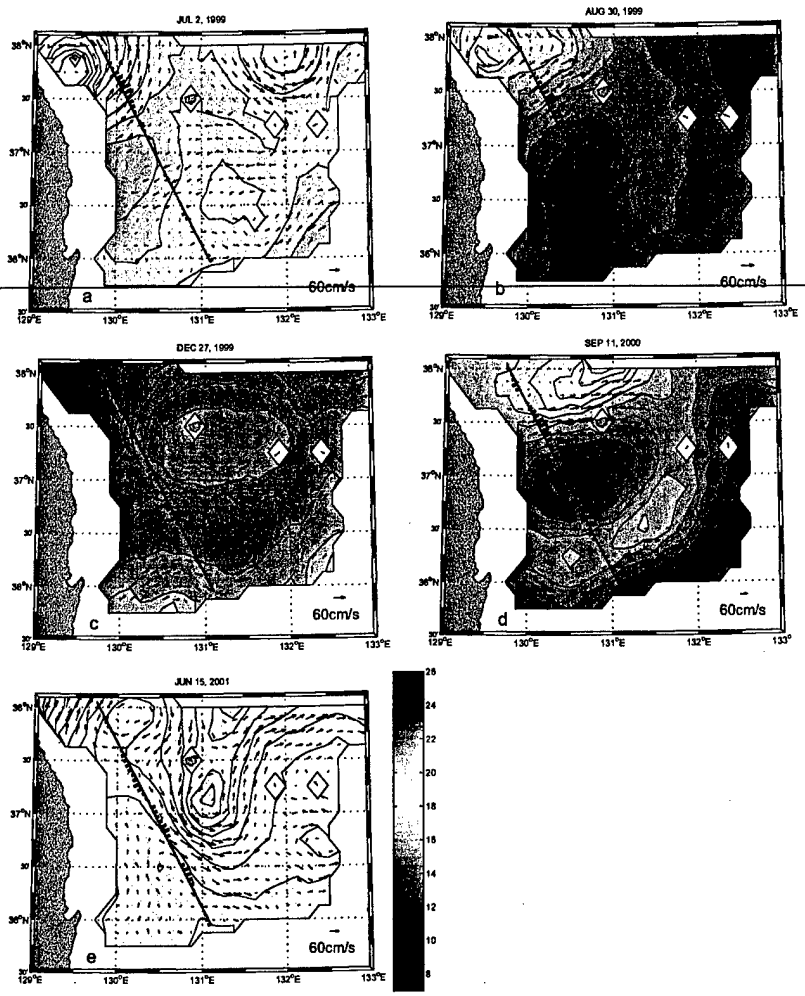

Fig. 7. Surface currents (arrows) and temperature at 100 m (colored background) produced from the PIES data and geostrophic velocities along T/P 112 are shown for (a) July 2, 1999, (b) August 30, 1999, (c) December 27, 1999, (d) September 11, 2000, and (e) June 15, 2001.

ple, the June 15, 2001 map (Fig. 7(e)) shows this meander whose warm source must be the EKWC. The T/P section shows the positive flow between about 36.2°N and 37°N that is associated with this meander of the EKWC.

The insight gained from understanding a T/P transect by comparison with the PIES maps can guide our interpretation of altimeter measurements for the full duration of the T/P mission since 1993. In this analogous way, in Fig. 4, the EKWC, UWE, and OB are identified for the full T/P time period. The absence of the EKWC and intensification of the OB that we verified directly in the year 2000 is similarly identified in 1993–1994 and in 1996 since the T/P section also shows OB strengthening during these time periods. The OB is absent during large portions of 1994, 1997, 1998, 1999, and 2001. A strong UWE period, similar to 1999–2001 also occurs at the beginning of the T/P section, 1993–1994. Smaller and weaker UWE periods are suggested throughout the rest of the T/P section. In addition, intensification of the EKWC is observed during the fall season from 1993 to 1998, and in 2001.

4. Discussion

Current analyses along individual T/P tracks provide a one-dimensional but spatially well-resolved perspective, which may be masked in the commonly performed two-dimensional objective analysis mapping of T/P data onto an (x, y) grid with resolution on the order of 100 km. Real features with scales on the order of tens of kilometers would be revealed in the former analysis but would be overly smoothed in the latter. However, overcoming the one-dimensional limitation to understand the features

along track requires an interpretation of the patterns that has generally required three-dimensional arrays of in situ measurements or otherwise insightful deduction of processes from more limited measurements. Two years of PIES measurements in the Ulleung Basin provide an unprecedented data set for combined analyses with altimetry.

Currents during the PIES recording period of two years (June, 1999 to July 2001) represent nearly the full range of observed anomalous patterns during the full T/P decade. Currents in the Ulleung Basin undergo large seasonal as well as extreme interannual fluctuations. The different current regimes can be illustrated by dividing the T/P current section into three bands (Band 1: southern edge to 36.25°N, Band 2: 36.25°N to 37.25°N, and Band 3: 37.25°N to northern edge) and computing average velocities in each band (Fig. 8). From 1999–2001, Band 2 average velocities are generally more negative and Band 3 average velocities are generally more positive. Such a pattern is characteristic of intensification of the UWE, clearly a dominant process during the PIES recording period. Negative velocities also occur in Band 2 during parts of 1993, 1995, and 1996 with corresponding positive peaks in Band 3 average velocities, except for 1996. In 1996, the UWE appears weakest. In addition, large OB peaks (positive velocities) can be seen in Band 1 in 1994, 1996, and 2000. Strong summer-fall seasonal peaks in average velocities are observed in Band 2 in 1994 to 1998 and in 2001.

The UWE is observed in the T/P current section for much of the PIES recording period (1999–2001). Approximating the location of the eddy along track by the zero velocity within the eddy signatures (Fig. 4) results in an eddy range from about 36.5°N to 37.8°N with the eddy center generally located near 37°N. In contrast, the UWE is not persistent throughout the nine-year T/P period, but instead forms for periods less than a year and then disappears, except for an extended eddy period from 1999 to 2001. During this period, the UWE remained large except for about a month at the beginning of 2000 when the UWE shrank in size, while approximately centered near Ulleung Island, but then recovered quickly to expand throughout much of the basin. Using repeated hydrographic stations between 1967 and 1986, An *et al.* (1994) found a similar position range and noted that the most frequently observed UWE position was between 37.0°N to 37.55°N, 130.0°E to 131.0°E. T/P 112 is well within this range. Using satellite-tracked drifters, from November 1992 through September 1993, Lie *et al.* (1995) observed the UWE continuously near 36.8°N, 130.6°E. The UWE is similarly observed along the T/P section at approximately this location and time period. Using four years of CREAMS hydrographic data, Kim *et al.* (1999) found considerable year-to-year temperature and salinity variability above the thermocline in the Ulleung Basin.

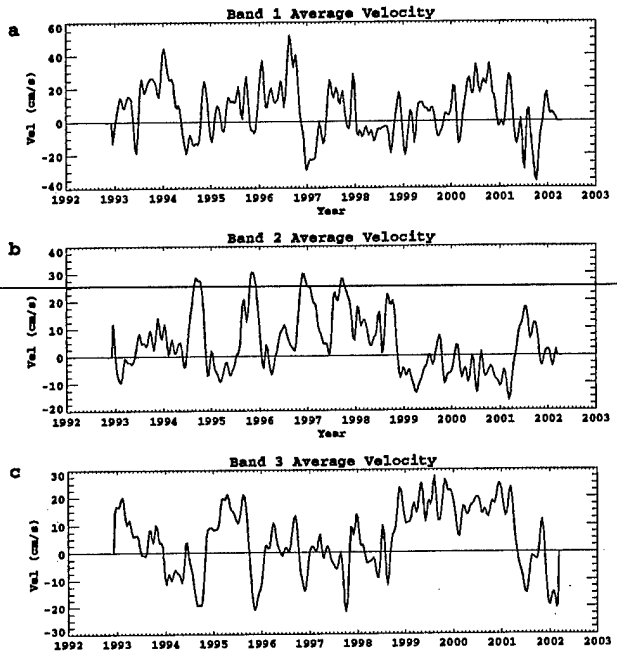

Fig. 8. Average velocities along T/P 112 from 1993 to 2002 for (a) band 1 (35.9°N to 36.25°N), (b) band 2 (36.25°N to 37.25°N), (c) band 3 (37.25°N to 38.1°N). Positive velocities are towards the northeast and negative velocities are towards the southwest.

They found salinity to be much lower in the summer of 1993 than in the summer of 1994. The T/P current section suggests an absence of the EKWC and large UWE formation in 1993, and a return of the EKWC in 1994. Such a current pattern would also result in the salinity pattern observed by Kim *et al.* (1999).

5. Conclusions

Absolute currents in the Ulleung Basin are derived using PIES measurements for the time period of 1993 through 2002 along T/P tracks. The height adjustments applied along the two T/P tracks in the Ulleung Basin are applicable for all times. Very good agreement is detected between absolute velocities calculated from PIES measurements with velocities calculated from altimetry data along T/P tracks.

The circulation patterns observed during 1999–2001 provided a new perspective on the circulation, differing qualitatively from the old paradigm of "three-current paths". Moreover, our observations differed qualitatively from the old concept of seasonally-repeated circulation patterns. Using nine years of T/P data provides the opportunity to view the 1999–2001 PIES measurements period in a broader temporal context and to examine the representativeness of the great variability and the circu-

lation patterns inferred along the T/P tracks. The three branch circulation pattern is neither a permanent nor a seasonally-repeating feature in the Ulleung Basin. Strong seasonal, annual, and interannual current and SSH variabilities are observed. The EKWC was strongest during summer–fall. In addition, the EKWC, UWE, and OB are interrupted intermittently, sometimes disappearing entirely, and therefore are difficult to map on an annual basis. Periods of strong OB appear to coincide with a weakened or absent EKWC. There are time periods dominated by the UWE, such as in 1999–2001. At other times the EKWC is more dominant, such as in 1996–1998. From 1993–1995, there is more of a mixture of EKWC and UWE. Circulation patterns in the Ulleung Basin changed throughout the nine-year analysis period. An annual cycle is not present but cycles can sometimes repeat for several years.

Similar high current variability is also likely in other regions of the world ocean and may be connected. Databases containing long-term ocean measurements over large areas, such as those from satellite altimetry, are required to understand ocean circulation. In situ measurements are essential for the correct interpretation of remotely sensed measurements. This study shows that even a decade of T/P observations alone (i.e., if lacking in situ data) is not enough to characterize interannual circulation patterns in the JES. Measurement systems (including both remotely sensed and in situ measurements) that continuously monitor ocean conditions are clearly needed to understand ocean dynamics and to establish connectivity.

Acknowledgements

This work was supported by the Office of Naval Research "Japan/East Sea DRI". Basic Research Programs include the Japan/East Sea initiative under grant N000149810246 and the Naval Research Laboratory's "Linkages of Asian Marginal Seas" under Program Element 0601153N.

References

An, H., K. Shim and H.-R. Shin (1994): On the warm eddies in the southwestern part of the East Sea (the Japan Sea). *J. Korean Soc. Oceanogr.*, **29**, 152–163.

Beardsley, R. C., R. Limeburner, K. Kim and J. Candela (1992): Lagrangian flow observations in the East China, Yellow and Japan Seas. *La Mer*, **30**, 297–314.

Byun, S.-K. and S.-D. Chang (1984): Two branches of Tsushima Warm Current in the Western Channel of the Korea Strait. *J. Oceanol. Soc. Korea*, **19**(2), 200–209.

Carnes, M. R., J. L. Mitchell and P. W. deWitt (1990): Synthetic temperature profiles derived from Geosat altimetry: comparisons with air-dropped expendable bathythermograph profiles. *J. Geophys. Res.*, **95**(C10), 17,979–17,992.

Cartwright, D. E. and R. D. Ray (1991): Energetics of global ocean tides from Geosat altimetry. *J. Geophys. Res.*, **96**(C9), 16,897–16,912.

Cho, Y.-K. and K. Kim (1996): Seasonal variation of the East Korean Warm Current and its relation with the cold water. *La Mer*, **34**, 172–182.

Choi, B. H. (1999): Digital Atlas for Neighboring Seas of Korean Peninsula. Laboratory for Coastal and Ocean Dynamics Studies, Sung Kyun Kwan University, CDROM.

Egawa, T., Y. Nagata and S. Sato (1993): Seasonal variation of the Current in the Tsushima Strait deduced from ADCP data of ship-of-opportunity. *J. Oceanogr.*, **49**, 39–50.

Fox, D. N., W. J. Teague, C. N. Barron, M. R. Carnes and C. M. Lee (2002): The Modular Ocean Data Assimilation System (MODAS). *J. Atmos. Ocean. Tech.*, **19**, 240–252.

Fu, L.-L., E. J. Christensen, C. A. Yamarone, Jr., M. Lefebvre, Y. Menard, M. Dorrer and P. Escudier (1994): TOPEX/POSEIDON mission overview. *J. Geophys. Res.*, **99**(C12), 24,369–24,381.

Hase, H., J.-H. Yoon and W. Koterayama (1999): The current structure of the Tsushima Warm Current along the Japanese coast. *J. Oceanogr.*, **55**, 217–235.

Hirose, N. and A. G. Ostrovskii (2000): Quasi-biennial variability in the Japan Sea. *J. Geophys. Res.*, **105**(C6), 14,011–14,027.

Hong, C.-H., K.-D. Cho and S.-K. Yang (1984): On the abnormal cooling phenomenon in the coastal areas of East Sea of Korea in summer, 1981. *J. Oceanol. Soc. Korea*, **19**, 11–17.

Ichiye, T. and K. Takano (1988): Mesoscale eddies in the Sea of Japan. *La Mer*, **26**, 69–79.

Isobe, A., S. Tawara, A. Kaneko and M. Kawano (1994): Seasonal variability in the Tsushima Warm Current, Tsushima-Korea Strait. *Cont. Shelf Res.*, **14**, 23–35.

Isobe, A., M. Ando, T. Watanabe, T. Senjyu, S. Sugihara and A. Manda (2002): Freshwater and temperature transports through the Tsushima-Korea Straits. *J. Geophys. Res.*, **107**(C7), Art. No. 3065Jul2002.

Kang, H. E. and Y. Q. Kang (1990): Spatio-temporal characteristics of the Ulleung Warm Lens. *Bull. Korean Fish. Soc.*, **203**, 407–415.

Katoh, O. (1994): Structure of the Tsushima Current in the southwestern Japan Sea. *J. Oceanogr.*, **50**, 317–338.

Katoh, O., K. Teshima, K. Kubota and K. Tsukiyama (1996): Downstream transition of the Tsushima Current west of Kyushu in summer. *J. Oceanogr.*, **52**, 93–108.

Kawabe, M. (1982a): Branching of the Tsushima Current in the Japan Sea, Part I. Data analysis. *J. Oceanogr. Soc. Japan*, **38**, 95–107.

Kawabe, M. (1982b): Branching of the Tsushima Current in the Japan Sea, Part II. Numerical experiment. *J. Oceanogr. Soc. Japan*, **38**, 183–192.

Kim, K. and R. Legeckis (1986): Branching of the Tsushima Current in 1981–1983. *Prog. Oceanogr.*, **17**, 256–276.

Kim, K., K.-R. Kim, J. Chung, H. Yoo and S. Park (1991): Characteristics of physical properties in the Ulleung Basin. *J. Oceanol. Soc. Korea*, **26**, 83–100.

Kim, K., Y.-G. Kim, Y.-K. Cho, M. Takematsu and Y. Volkov (1999): Basin-to-basin and year-to-year variation of temperature and salinity characteristics in the East Sea (Sea of

Japan). *J. Oceanogr.*, **55**, 103–109.
Lee, D.-K, P. P. Niiler, S.-R. Lee, K. Kim and H.-J. Lie (2000): Energetics of the surface circulation of the Japan/East Sea. *J. Geophys. Res.*, **105**, 19,561–19,573.
Lie, H.-J., S.-K. Byun, I. Bang and C.-H. Cho (1995): Physical structure of eddies in the southwestern East Sea. *J. Korean Soc. Oceanogr.*, **30**, 170–183.
Meinen, C. and D. R. Watts (2000): Vertical structure and transport on a transect across the North Atlantic Current near 42 degrees N: time series and mean. *J. Geophys. Res.*, **105**, 21,869–21,891.
Mitchell, D. A., D. R. Watts, M. Wimbush, K. L. Tracey, W. J. Teague, J. W. Book, K.-I. Chang, M.-S. Suk and J.-H. Yoon (2004a): Upper circulation patterns in the Ulleung Basin. *Deep-Sea Res.* (accepted).
Mitchell, D. A., M. Wimbush, D. R. Watts and W. J. Teague (2004b): The residual GEM technique and its application to the southwestern Japan/East Sea. *J. Atmos. Ocean. Tech.* (accepted).
Mitchell, J. L., J. M. Dastugue, W. J. Teague and Z. R. Hallock (1990): The estimation of geoid profiles in the NW Atlantic from simultaneous satellite altimetry and AXBT sections. *J. Geophys. Res.*, **95**(C10), 17,965–17,977.
Mizuno, S., K. Kawatate, T. Nagahama and T. Miita (1989): Measurements of East Tsushima Current in winter and estimation of its seasonal variability. *J. Oceanogr. Soc. Japan*, **45**, 375–384.
Morimoto, A. and T. Yanagi (2001): Variability of sea surface circulation in the Japan Sea. *J. Oceanogr.*, **57**, 1–13.
Morimoto, A., T. Yanagi and A. Kaneko (2000): Eddy field in the Japan Sea derived from satellite altimetric data. *J. Oceanogr.*, **56**, 449–462.
Moriyasu, S. (1972): The Tsushima Current. p. 353–369. In *Kuroshio: Its Physical Aspects*, ed. by H. Stommel and K. Yoshida, University of Tokyo Press, Tokyo.
Naganuma, K. (1973): On discussions on the existence of the Third-Branch of the Tsushima current. *Jpn. Sea Reg. Fish. Res. Lab.*, **266**, 1–3 (in Japanese).
Naganuma, K. (1985): Fishing and oceanographic conditions in the Japan Sea. *Umi to Sora*, **60**, 89–103 (in Japanese).
Schrama, E. J. O. and R. D. Ray (1994): A preliminary tidal analysis of TOPEX/POSEIDON altimetry. *J. Geophys. Res.*, **99**(C12), 24,799–24,808.
Schwiderski, E. W. (1980): On charting global ocean tides. *Rev. Geophys. Space Phys.*, **18**, 243–268.
Suda, K. and K. Hidaka (1932): The results of the oceanographical observations aboard R.M.S. Syunpu Maru in the southern part of the Sea of Japan in the summer of 1929, Part 1. *Journal of Oceanography Imperial Marine Observations*, **3**, 291–375 (in Japanese).
Teague, W. J., Z. R. Hallock and G. A. Jacobs (1997): Estimation of a geoid section across the Kuroshio. *J. Atmos. Ocean. Tech.*, **14**(2), 326–330.
Teague, W. J., G. A. Jacobs, H. T. Perkins, J. W. Book, K.-I. Chang and M.-S. Suk (2002): Low frequency current observations in the Korea Strait. *J. Phys. Ocean.*, **32**, 1621–1641.
Teague, W. J., P. A. Hwang, G. A. Jacobs, J. W. Book and H. T. Perkins (2003): Transport variability across the Korea/Tsushima Strait and the Tsushima Island Wake. *Deep-Sea Res.* (accepted).
Uda, M. (1934): The results of simultaneous oceanographical investigations in the Japan Sea and its adjacent waters in May and June, 1932. *Japan Imperial Fishery Experiment Stations*, **5**, 57–190 (in Japanese).
Watts, D. R., C. Sun and S. Rintoul (2001): A 2-d gravest empirical mode determined from hydrographic observations in the subantarctic front. *J. Phys. Ocean.*, **31**, 2186–2209.
Yoon, J. H. (1982a): Numerical experiment on the circulation in the Japan Sea, Part 1. Formation of the East Korean Warm Current. *J. Oceanogr. Soc. Japan*, **38**, 38–43.
Yoon, J. H. (1982b): Numerical experiment on the circulation in the Japan Sea, Part 3. Mechanism of the nearshore branch of the Tsushima Current. *J. Oceanogr. Soc. Japan*, **38**, 125–130.